 doi:10.20944/preprints201803.0088.v1

Article

Integrating Monte Carlo and the Hydrodynamic Model for Predicting Extreme Water Levels in River Systems

Wen-Cheng Liu [1,*] and Hong-Ming Liu [1]

[1] Department of Civil and Disaster Prevention Engineering, National United University, Miaoli 36063, Taiwan; wcliu@nuu.edu.tw; dslhmd@gmail.com
* Correspondence: wcliu@nuu.edu.tw; Tel.: +886-37-38235

Abstract: Estimates of extreme water level return periods in river systems are crucial for hydraulic engineering design and planning. Recorded historical water level data of Taiwan's rivers are not long enough for traditional frequency analyses when predicting extreme water levels for different return periods. In this study, the integration of a one-dimensional flash flood routing hydrodynamic model with the Monte Carlo simulation was developed to predict extreme water levels in the Danshuei River system of northern Taiwan. The numerical model was calibrated and verified with observed water levels using four typhoon events. The results indicated a reasonable agreement between the model simulation and observation data. Seven parameters, including the astronomical tide and surge height at the mouth of the Danshuei River and the river discharge at five gauge stations, were adopted to calculate the joint probability and generate stochastic scenarios via the Monte Carlo simulation. The validated hydrodynamic model driven by the stochastic scenarios was then used to simulate extreme water levels for further frequency analysis. The design water level was estimated using different probability distributions in the frequency analysis at five stations. The design high-water levels for a 200-year return period at Guandu Bridge, Taipei Bridge, Hsin-Hai Bridge, Da-Zhi Bridge, and Chung-Cheng Bridge were 2.90 m, 5.13 m, 6.38 m, 6.05 m, and 9.94 m, respectively. The estimated design water levels plus the freeboard are proposed and recommended for further engineering design and planning.

Keywords: extreme water level, hydrodynamic model, Monte Carlo, joint probability, model calibration and verification, Danshuei River system

1. Introduction

Extreme water levels in tidal rivers can cause overbanking and levee breaking, which results in economic and human life losses and social impacts. The water level in this type of transitional area is affected by upstream river flow, downstream tidal levels, and the operation of existing controllable structures [1]. Tidal rivers have negative impacts on surrounding areas where residents live, but these rivers also contribute several benefits. The astronomical tide at the mouth of tidal rivers obstructs fluvial flows flowing towards downstream reaches. The water level increases due to the interaction between tides and floods in tidal rivers [2,3]. Moreover, it is vital to assess extreme water level frequency for flood risks and future flood defense designs. The resistance of river levees against flooding is captured in the design water level.

There are two major approaches when determining extreme water levels depending on the availability of the observed water level data at a site. The first approach is a numerical simulation method. It can be used when there is not an adequate observational record for flooded water levels. A hydrodynamic model provides the link between the known statistics of the generating forces and the desired statistics of the water levels. These simulation methods, such as the joint probability method [4,5] and the Monte Carlo simulation [6], can be used to accurately predict extreme water levels. The second approach is a frequency analysis of annual maximum water levels that results from the combination of several forcing factors [7,8]. This approach can be used when reasonably

 doi:10.20944/preprints201803.0088.v1

long observation data (greater than 60 years) are available [9,10]. Xu and Huang [11] used a 91-year data set at the Wusong station near Shanghai in the Yangtze estuary to estimate the 100-year annual maximum water level (AMWL) using a general extreme value (GEV) model to support coastal hazard mitigation planning. To examine the effect of a shorter data set, a 59-year data set was investigated. They found that model predictions using the 59-year data set underestimated the observed 60-year AMWL.

It is difficult to find long-term datasets greater than 60 years from gauge stations at Taiwanese river mouths. Therefore, a traditional frequency analysis is not appropriate for gauge stations in Taiwan. The alternative numerical simulation method is suitable for analyzing extreme water levels. This method can be used to simulate extreme water levels using a hydrodynamic model driven by discharge upriver and tidal levels at the river mouth. The hydrodynamic model provides a link between a generating forcing with a return period and the expected extreme water levels. Mantz and Wakeling [12] and Samuels and Burt [13] used a very limited number of sampling scenarios, but they adopted accurate Monte Carlo simulations to produce a very large number of stochastic sampling scenarios. A simplified one-dimensional hydrodynamic model of the lower Rhine delta was applied to simulate extreme water levels. Zhong et al. [6] established a joint probability analysis on astronomical tides, wind-induced storm surge, the Rhine flow and the Muse flow at the river boundaries to produce a joint probability distribution. A one-dimensional hydrodynamic model was then applied to estimate high water-level frequencies in the estuary delta. The sampled Monte Carlo simulation method was used to generate a large number of stochastic scenarios as inputs for the one-dimensional hydrodynamic model.

Rivers in Taiwan are short with steep slope and meandering that is favorable to the occurrence of flooding at midstream/downstream reaches when heavy rainfalls occur in the basin during typhoon events. In recent years, the rapid urbanization without sufficient floodplain management resulted in highly developed and densely populated zones over riversides. The existent hydraulic facilities were unable to provide enough flood protection. Therefore, flooding is one of the worst natural hazards causing serious economic and social impacts in Taiwan [14,15].

The objective of this study is to integrate a one-dimensional flash flood routing hydrodynamic model with a Monte Carlo simulation to estimate extreme water levels in the Danshuei River system of northern Taiwan. The hydrodynamic model was first calibrated and verified with measured water levels using several typhoon events. The validated model was then applied to calculate water levels in the river system. Different water level scenarios at the downstream boundary and discharges at upstream boundaries were yielded from the Monte Carlo simulation to drive the hydrodynamic model. The desired extreme water levels with return periods of 50, 100, and 200 years are proposed in this study.

2. Materials and Methods

2.1. Description of Study Site

The Danshuei River system is located in northern Taiwan (Figure 1). It covers three major tributaries, the Dahan River, the Xindian River, and the Keelung River, and its watershed has a population of over six million people [16]. Therefore, effective management and flood control of the Danshuei River system is one of the most important tasks in Taiwan. The Erchung flood diversion channel, built near the confluence of the Dahan River and the Xindian River in 1984, was used to divert flood flow during typhoon events. The Danshuei watershed area is 2,726 km^2, with a mean annual precipitation of 3001 mm. The total channel length is 327.6 km, and the channel slope ranges from 0.015° to 0.0027°. The peak discharge of a 200-year flood reaches 25,000 m^3/s. The major forcing mechanisms of flood flows are astronomical tides at the river mouth and river discharges at the upriver boundary. Semi-diurnal tides are represented by principal tidal constituents, with a mean tidal range of 2.21 m and a spring tidal range of 3.1 m. The downstream reaches of all three tributaries are affected by tides [17,18].

Preprints (www.preprints.org) | NOT PEER-REVIEWED | Posted: 12 March 2018 doi:10.20944/preprints201803.0088.v1

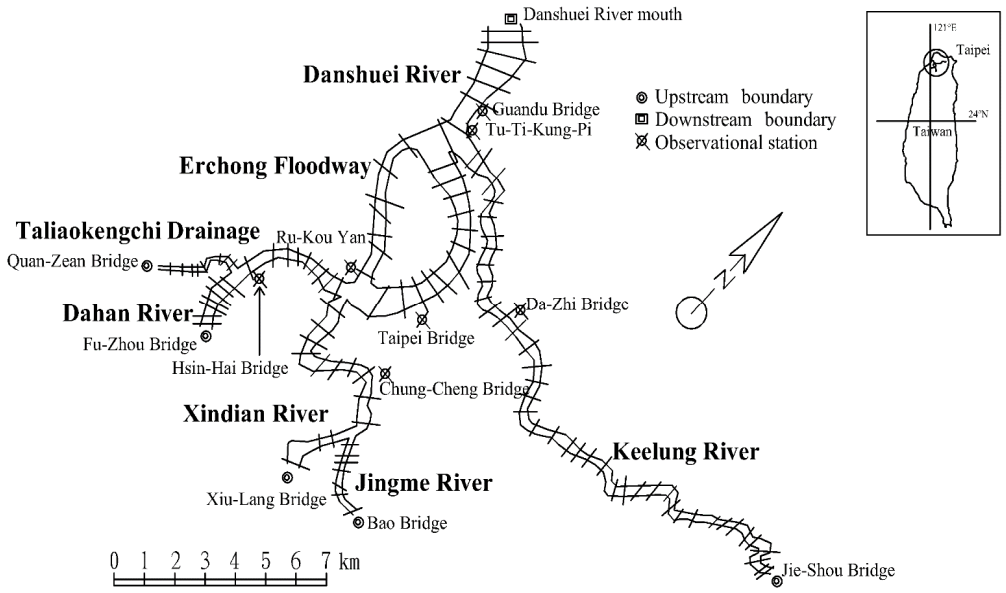

Figure 1. Map of the Danshuei River system in northern Taiwan.

2.2. Governing Equations of the One-Dimensional Model

The flash flood routing hydrodynamic model is based on a dynamic wave theory using Saint-Venant equations, which consist of one-dimensional continuity and momentum equations:

$$\frac{\partial A}{\partial t}+\frac{\partial Q}{\partial x}-q_1+q_2+q_3=0 \quad (1)$$

$$\frac{\partial Q}{\partial t}+\frac{\partial}{\partial x}\left(\frac{Q^2}{A}\right)-gA\left(S_o-\frac{\partial Y}{\partial x}-S_f\right)-q_1V_1+q_2\left(\frac{Q}{A}\right)+q_3\left(\frac{Q}{A}\right)=0 \quad (2)$$

where A represents the cross-sectional area, Y represents the water depth, Q represents the discharge, q_1 represents the lateral inflow per unit channel length, q_2 represents the levee-break flow per unit channel length, q_3 represents the lateral outgoing overbank flow per unit channel length, S_0 represents the bottom slope of the channel, S_f represents the friction slope, V_1 represents the longitudinal velocity component of the lateral inflow, g represents the gravitational acceleration, t represents time, and x represents the distance along the channel. Because the cross-sectional area can be written as a function of water depth, only two flow variables, Q and Y, must be solved in Eqs. (1) and (2). The four-point implicit finite difference approximation scheme [19,20] was used in this study to solve for variables Q and Y. The detailed algorithms of the solution can be found in Liu and Wu [21].

2.3. Hydrodynamic Model Setup

In this study, the model transects were established with measured cross-sectional profiles at approximately 0.5 km intervals along the river. The model transects in the computational domain included 310 transects and covered 11 river reaches (shown in Table 1). The upstream boundaries are specified at Fu-Zhou Bridge (Dahan River), Quan-Zean Bridge (Taliaokengchi drainage, which is a tributary of the Dahan River), Xiu-Lang Bridge (Xindian River), Bao Bridge (Jingme River, which is a tributary of the Xindian River), and Jie-Shou Bridge (Keelung River). The downstream boundary is located at the mouth of the Danshuei River. The upstream and downstream boundaries are shown in Figure 1. The upstream boundary conditions of the dynamic flood routing hydrodynamic model are represented by the discharges and tidal levels specified at the mouth of the Danshuei River (Figure 1). Figure 2 illustrates the layout of the Danshuei River system for model simulation.

Preprints (www.preprints.org) | NOT PEER-REVIEWED | Posted: 12 March 2018 doi:10.20944/preprints201803.0088.v1

Table 1. Cross-sectional number of river reaches and Manning coefficients (n) used in the computational domain.

River reach number	1	2	3	4	5	6
Number of cross section	71	8	3	13	9	22
Manning friction n	0.025	0.033	0.035	0.040	0.033	0.027
River reach number	7	8	9	10	11	
Number of cross section	22	10	2	137	13	
Manning friction n	0.033	0.033	0.033	0.050	0.023	

Table 2. Data description.

Station	Data	Time	Data description
Danhuei River mouth	Observed tidal level	1994~2015	Hourly tidal level
Quan-Zean Bridge (Taliaokengchi Drainage)	Observed river discharge	1994~2014	Daily-average discharge
Fu-Zhou Bridge (Dahan River)	Observed river discharge	1994~2014	Daily-average discharge
Xiu-Lang Bridge (Xindian River)	Observed river discharge	1994~2014	Daily-average discharge
Bao Bridge (Jingme River)	Observed river discharge	1994~2014	Daily-average discharge
Jie-Shou Bridge (Keelung River)	Observed river discharge	1994~2014	Daily-average discharge

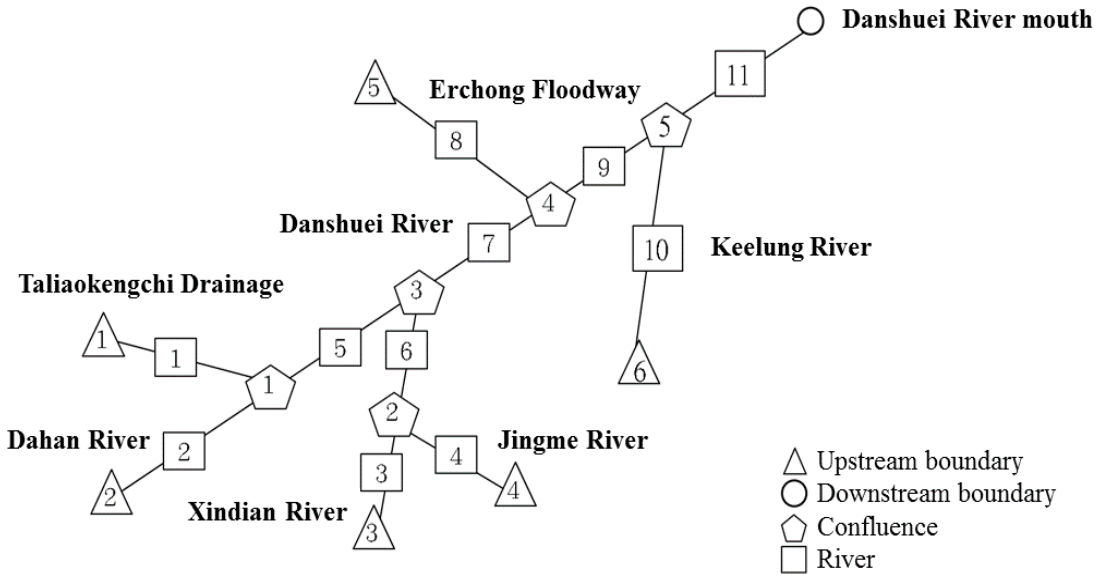

Figure 2. Layout of the Danshuei River system for the model simulation.

2.4. Data Collection and Analysis

Observational data, including tidal levels at the mouth of the Danshuei River and discharges upstream of the Taliaokengchi drainage, Dahan River, Xindian River, Jiangme River, and Keelung

Preprints (www.preprints.org) | NOT PEER-REVIEWED | Posted: 12 March 2018 doi:10.20944/preprints201803.0088.v1

River, were collected from the Water Resource Agency of Taiwan. The data are shown in Table 2. Surge heights during typhoon periods were calculated as the difference between the observed tidal level and the astronomical tide. Observational data for astronomical tides, surge heights, and discharges were used to analyze and yield the probability of each parameter.

2.5. Frequency Analysis Methods

Several researchers have used frequency analyses to investigate extreme water levels [22-24]. For example, the Federal Emergency Management Agency (FEMA) recommends the use of the GEV model for extreme value analyses of annual maxima to investigate coastal flood insurance along the west coast of the USA near the Pacific Ocean [25]. There are many peer-reviewed articles regarding the application of GEV distributions described by a shape factor parameter [9,26,27]. However, other types of probability distributions for frequency analyses should be used to select the best distribution for extreme values. In this study, different types of distributions were used to analyze extreme values. Table 3 shows the frequency analysis probability distributions for extreme values, including the Gumbel, Weibull, Frechet, normal, lognormal, and log-Pearson 3 distributions.

The standard error (SE) and the correlation coefficient (CC) were used as indicators when evaluating the performance of each extreme value distribution. The most adaptive distribution (i.e., the lowest SE and the highest CC) will be selected for further applications. The expressions for the SE and the CC are given as follows:

$$SE = \sqrt{\frac{\sum_{i=1}^{n} (x_i - \hat{x}_i)^2}{n}} \tag{3}$$

$$CC = \frac{\sum_{i=1}^{n} \left(x_i - \bar{x}\right)\left(\hat{x}_i - \bar{\hat{x}}\right)}{\sqrt{\sum_{i=1}^{n} \left(x_i - \bar{x}\right)^2} \sqrt{\sum_{i=1}^{n} \left(\hat{x}_i - \bar{\hat{x}}\right)^2}} \tag{4}$$

where x_i represents the observed value, $\hat{x}_i$ represents the estimated value, $\bar{x}$ represents the mean of the sampling data, $\bar{\hat{x}}$ represents the mean of the estimated data, and n represents the number of data.

2.6. Monte Carlo Simulation

Monte Carlo methods are a broad class of computational algorithms that rely on repeated random sampling to obtain numerical results. The essential idea is the use of randomness to solve problems that might be deterministic in principle. They are often used in physical and mathematical problems and are most useful when it is difficult or impossible to use other approaches [28]. Monte Carlo simulations have been widely used in engineering for sensitivity analyses and quantitative probabilistic analyses in process design. For example, they are applied in coastal flood damage estimates and coastal hydrodynamic modeling [29-32], flood propagation modeling [33,34], rainfall hyetograph design [35], and water quality modeling [36-39].

In this study, a joint probability analysis of astronomical tides, surge heights, and river discharges at five upstream boundaries is established to produce a joint probability distribution of potential flood events. Then, importance sampling with the Monte Carlo simulation method is used to help generate a large number of stochastic scenarios as the inputs for the one-dimensional flash flood routing hydrodynamic model. A set of 2000 scenarios is generated from the Monte Carlo simulations to compute extreme water levels in a river system.

Preprints (www.preprints.org) | NOT PEER-REVIEWED | Posted: 12 March 2018 doi:10.20944/preprints201803.0088.v1

Table 3. Probability distributions for the frequency analysis of extreme values.

Probability model	Range	$f(x)$=PDF $F(x)$=CDF
Gumbel	$-\infty < x < +\infty$; $\sigma > 0$	$f(x) = \frac{1}{\sigma}\exp(-(\frac{x-\mu}{\sigma}) - \exp(-(\frac{x-\mu}{\sigma})))$ $F(x) = \exp(-\exp(-(\frac{x-\mu}{\sigma})))$
Weibull	$\gamma \le x < +\infty$; $\alpha, \beta > 0$	$f(x) = \frac{\alpha}{\beta}\left(\frac{x-\gamma}{\beta}\right)^{\alpha-1}\exp\left(-\left(\frac{x-\gamma}{\beta}\right)^{\alpha}\right)$ $F(x) = 1-\exp\left(-\left(\frac{x-\gamma}{\beta}\right)^{\alpha}\right)$
Frechet	$\gamma < x < +\infty$; $\alpha, \beta > 0$	$f(x) = \frac{\alpha}{\beta}\left(\frac{\beta}{x-\gamma}\right)^{\alpha+1}\exp\left(-\left(\frac{\beta}{x-\gamma}\right)^{\alpha}\right)$ $F(x) = \exp\left(-\left(\frac{\beta}{x-\gamma}\right)^{\alpha}\right)$
Normal	$-\infty < x < +\infty$; $\sigma > 0$	$f(x) = \frac{\exp\left(-\frac{1}{2}\left(\frac{x-\mu}{\sigma}\right)^2\right)}{\sigma\sqrt{2\pi}}$ $F(x) = \Phi\left(\frac{x-\mu}{\sigma}\right)$
Lognormal	$\gamma < x < +\infty$; $\sigma, \mu > 0$	$f(x) = \frac{\exp\left(-\frac{1}{2}\left(\frac{\ln(x-\gamma)-\mu}{\sigma}\right)^2\right)}{(x-\gamma)\sigma\sqrt{2\pi}}$ $F(x) = \Phi\left(\frac{\ln(x-\gamma)-\mu}{\sigma}\right)$
Log-Pearson 3	$0 < x \le e^{\gamma}$ $\beta < 0$; $e^{\gamma} \le x < +\infty$ $\beta > 0$; $\alpha > 0, \beta \ne 0$	$f(x) = \frac{1}{x\lvert\beta\rvert\Gamma(\alpha)}\left(\frac{\ln(x)-\gamma}{\beta}\right)^{\alpha-1}\exp\left(-\frac{\ln(x)-\gamma}{\beta}\right)$ $F(x) = \frac{\Gamma_{(\ln(x)-\gamma)/\beta}(\alpha)}{\Gamma(\alpha)}$

Note: PDF: Probability density function; CDF: Cumulative density function

2.7. Indices of the Hydrodynamic Simulation Performance

To evaluate the performance of the one-dimensional flash flood routing hydrodynamic model, two criteria were used to compare the simulated results and the measured data: the mean absolute error (MAE) and the root mean square error (RMSE). The error indices can be defined by Eqs. (5) and (6), respectively:

$$MAE = \frac{1}{N}\sum_{i=1}^{N}\left|H_{sim,i} - H_{mes,i}\right| \quad (5)$$

Preprints (www.preprints.org) | NOT PEER-REVIEWED | Posted: 12 March 2018 doi:10.20944/preprints201803.0088.v1

$$RMSE = \left[\frac{1}{N} \sum_{i=1}^{N} [H_{sim,i} - H_{mes,i}]^2 \right]^{1/2} \quad (6)$$

where H_{mes} represents the measured water level, H_{sim} represents the simulated water level, and N represents the number of time measurements.

3. Model Calibration and Verification

To ascertain the model accuracy for further practical applications, the observational data are used to calibrate and verify the model and to validate its capability when predicting water levels in the river system.

The friction coefficient (n) is an important parameter affecting the calculation of the water level in the Danshuei River system during flooding periods. Two typhoons events, Typhoon Krosa (2007) and Typhoon Fungwong (2008), were used for the model calibration, and two other typhoon events, Typhoon Saola (2012) and Typhoon Soulik (2013), were used for model verification. The tracks of these typhoon events are illustrated in Figure 3.

Figure 4 and Figure 5 present the calibration results for Typhoon Krosa (2007) and Typhoon Fungwong (2008), respectively. They indicate that the computed water level hydrograph is similar to the observed water level hydrograph. The mean absolute errors (MAEs) of the events at Taipei Bridge, Hsin-Hai Bridge, Da-Zhi Bridge, Chung-Cheng Bridge, Tu-Ti Kung Pi, and Ru-Kou Yan (locations are shown in Figure 1) during Typhoon Krosa are 0.30 m, 0.30 m, 0.23 m, 0.22 m, 0.23 m, and 0.33 m, respectively. In addition, the mean absolute errors (MAEs) of the events at Taipei Bridge, Hsin-Hai Bridge, Da-Zhi Bridge, Chung-Cheng Bridge, Tu-Ti Kung Pi, and Ru-Kou Yan during Typhoon Fungwong are 0.19 m, 0.15 m, 0.24 m, 0.22 m, 0.07 m, and 0.18 m, respectively. It can be seen that the calibrated results for Typhoon Fungwong are better than those for Typhoon Krosa.

Figure 6 and Figure 7 present the verification results for Typhoon Saola (2012) and Typhoon Soulik (2013), respectively. These figures also reveal that the computed water levels mimic the observed water levels at different gauge stations. The mean absolute errors (MAE) of the events at Taipei Bridge, Hsin-Hai Bridge, Da-Zhi Bridge, Chung-Cheng Bridge, Tu-Ti Kung Pi, and Ru-Kou Yan during Typhoon Saola are 0.24 m, 0.06 m, 0.21 m, 0.11 m, 0.17 m, and 0.40 m, respectively. In addition, the mean absolute errors (MAEs) of the events at Taipei Bridge, Hsin-Hai Bridge, Da-Zhi Bridge, Chung-Cheng Bridge, and Tu-Ti Kung Pi during Typhoon Soulik are 0.19 m, 0.18 m, 0.13 m, 0.17 m, and 0.10 m, respectively. There are no observational data at Rou-Kou Yan during Typhoon Soulik for model verification.

Table 1 presents the Manning friction coefficient (n) adopted in the model. Table 4 presents the MAE and RMSE values at each station for the four typhoon events. The results show a reasonable agreement between the model predictions and the measured data.

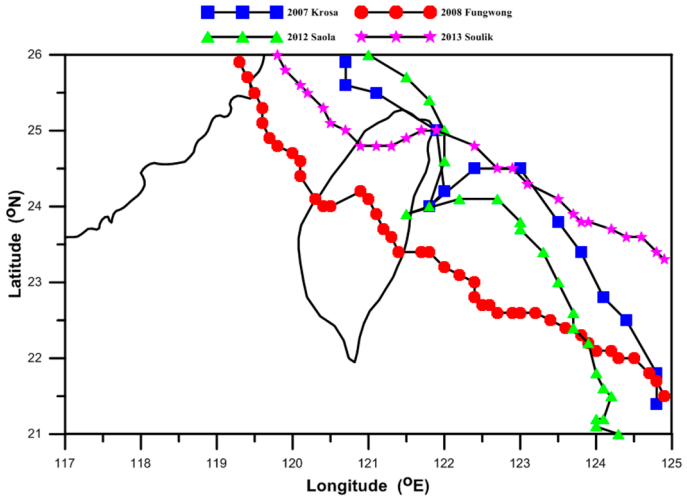

Figure 3. Paths of the four typhoon events.

Preprints (www.preprints.org) | NOT PEER-REVIEWED | Posted: 12 March 2018 doi:10.20944/preprints201803.0088.v1

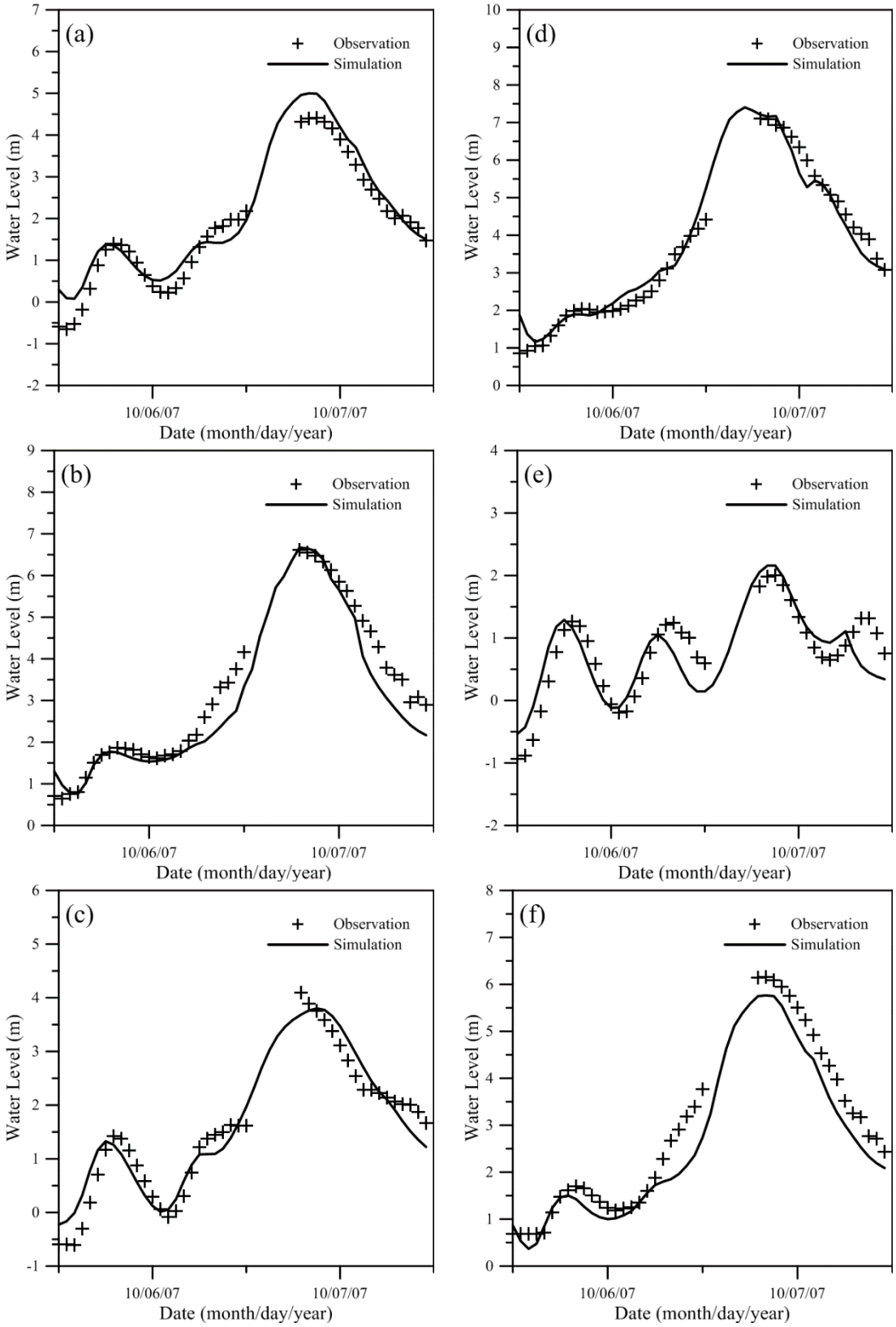

Figure 4. Model calibration results for Typhoon Krosa (2007) at (a) Taipei Bridge, (b) Hsin-Hai Bridge, (c) Da-Zhi Bridge, (d) Chung-Cheng Bridge, (e) Tu-Ti-Kung-Pi, and (f) Ru-Kou Yan.

Preprints (www.preprints.org) | NOT PEER-REVIEWED | Posted: 12 March 2018 doi:10.20944/preprints201803.0088.v1

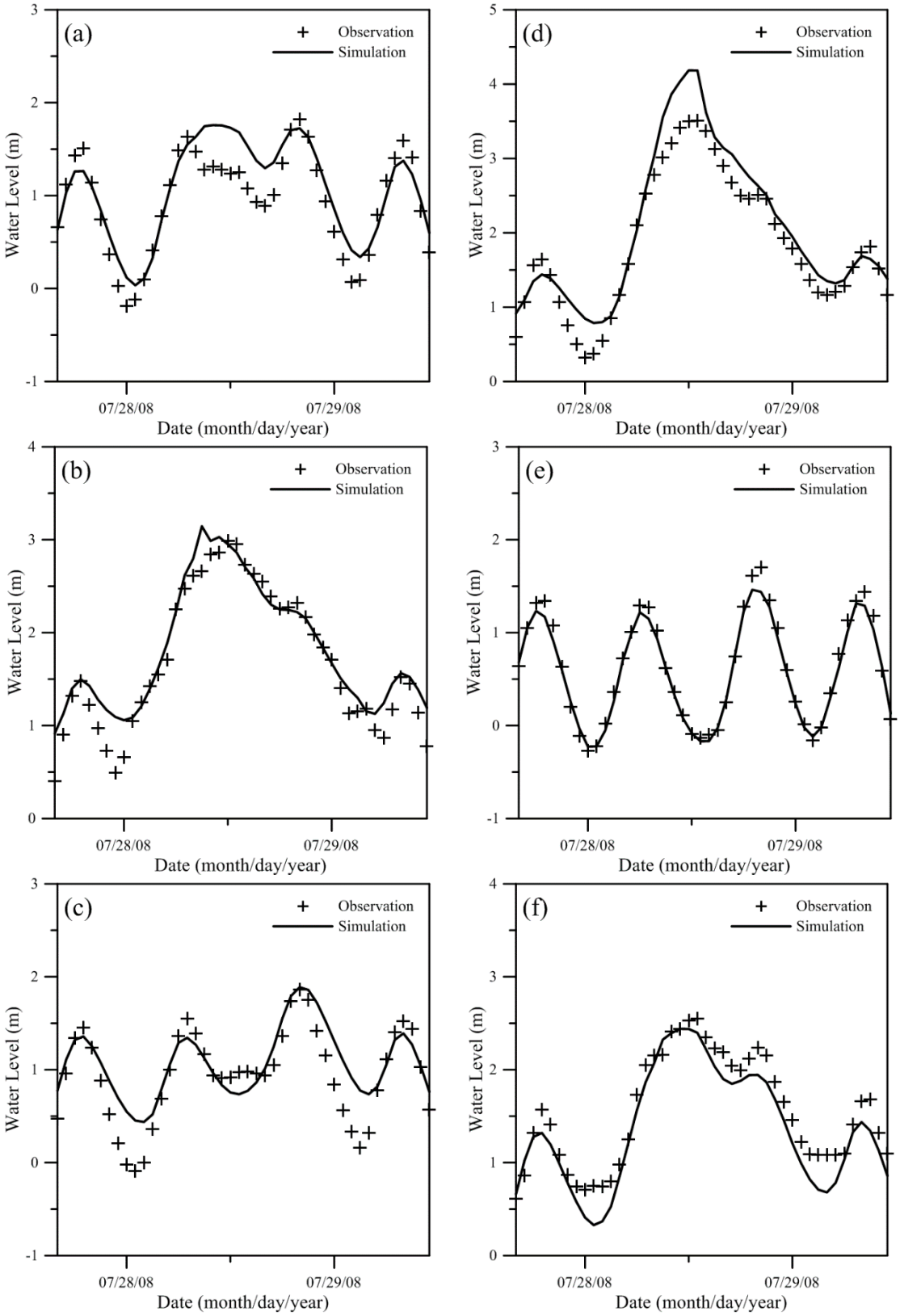

Figure 5. Model calibration results for Typhoon Fungwong (2008) at (a) Taipei Bridge, (b) Hsin-Hai Bridge, (c) Da-Zhi Bridge, (d) Chung-Cheng Bridge, (e) Tu-Ti-Kung-Pi, and (f) Ru-Kou Yan.

Preprints (www.preprints.org) | NOT PEER-REVIEWED | Posted: 12 March 2018 doi:10.20944/preprints201803.0088.v1

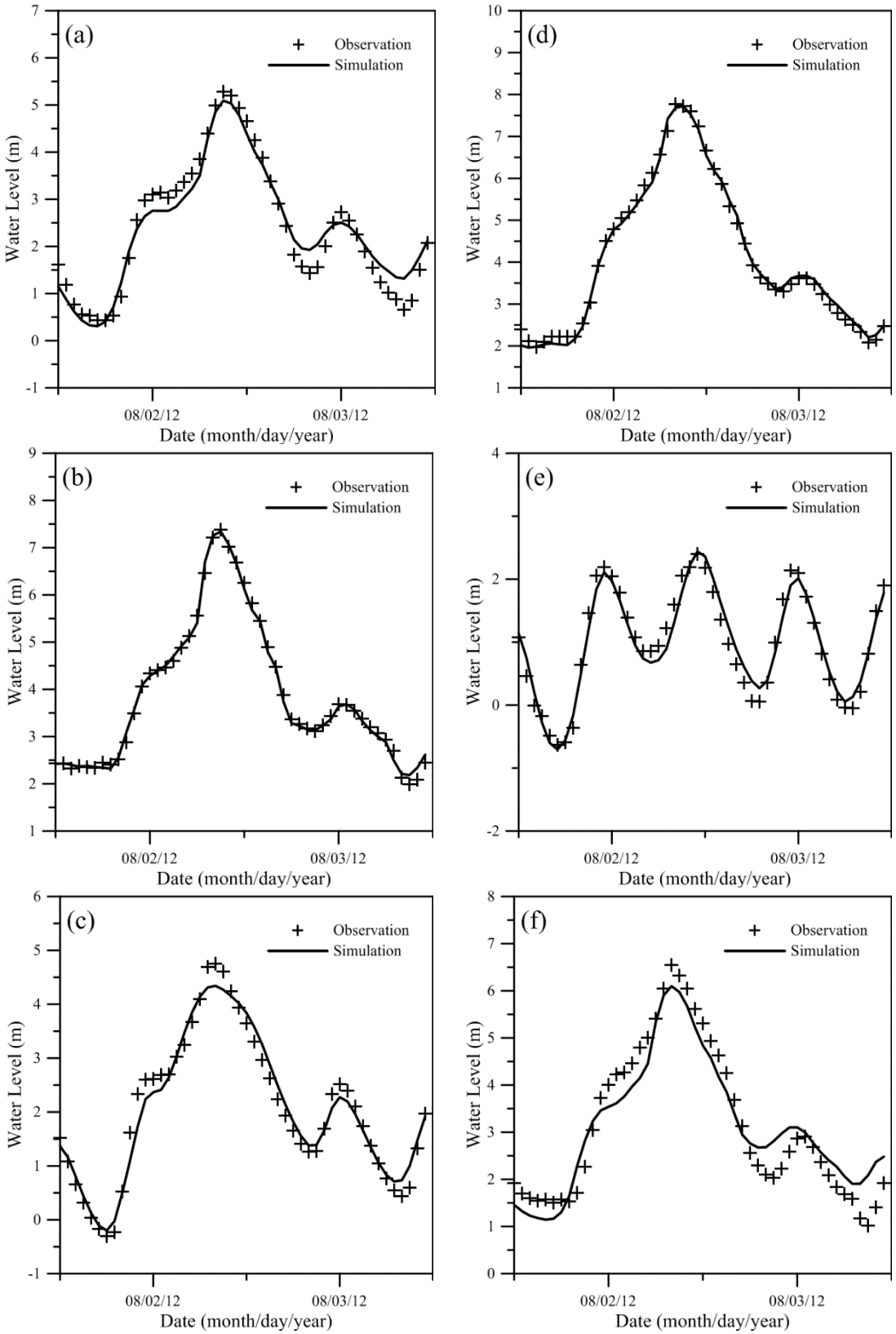

Figure 6. Model verification results for Typhoon Saola (2012) at (a) Taipei Bridge, (b) Hsin-Hai Bridge, (c) Da-Zhi Bridge, (d) Chung-Cheng Bridge, (e) Tu-Ti-Kung-Pi, and (f) Ru-Kou Yan.

Preprints (www.preprints.org) | NOT PEER-REVIEWED | Posted: 12 March 2018 doi:10.20944/preprints201803.0088.v1

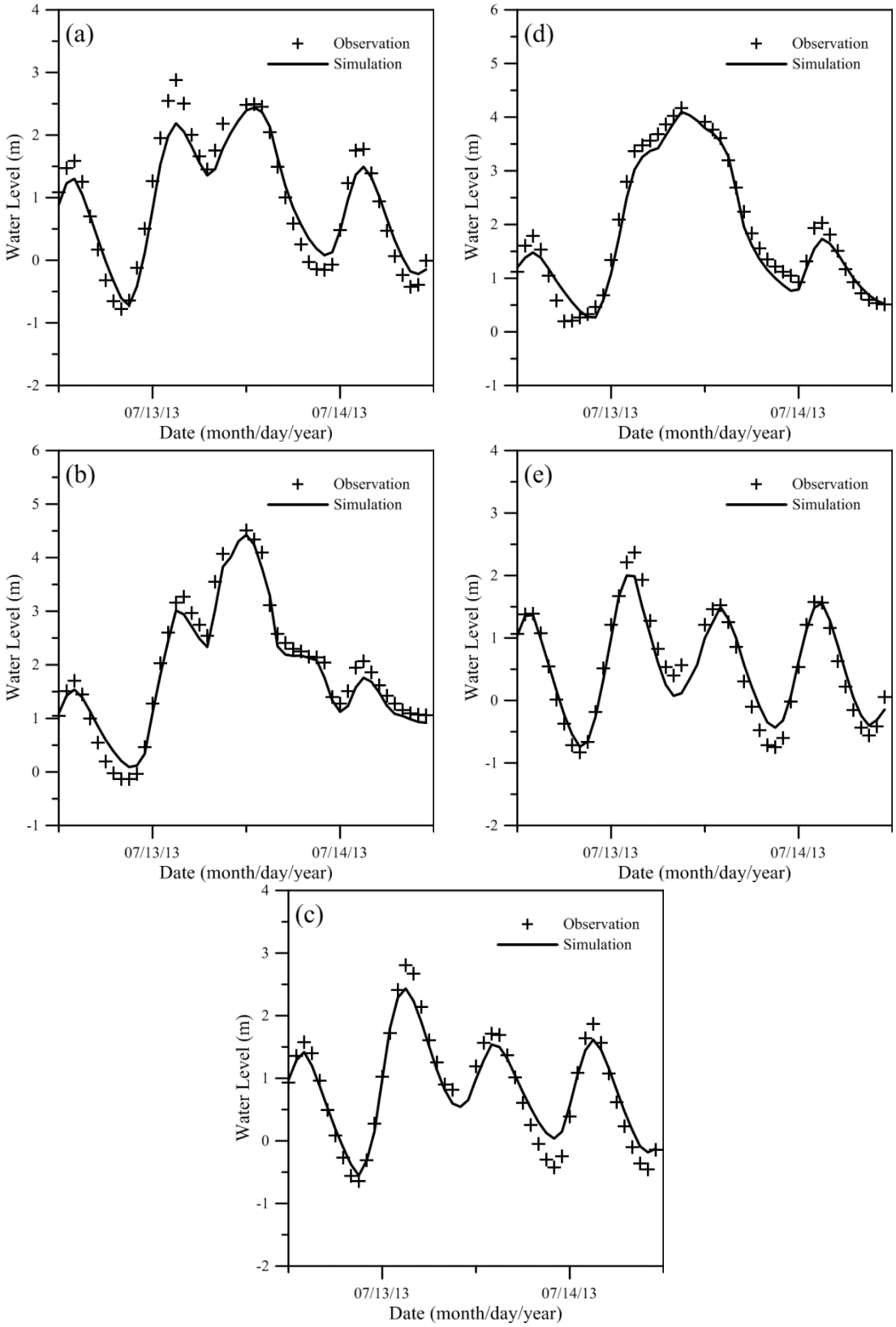

Figure 7. Model verification results for Typhoon Soulik (2013) at (a) Taipei Bridge, (b) Hsin-Hai Bridge, (c) Da-Zhi Bridge, (d) Chung-Cheng Bridge, and (e) Tu-Ti-Kung-Pi.

Preprints (www.preprints.org) | NOT PEER-REVIEWED | Posted: 12 March 2018 doi:10.20944/preprints201803.0088.v1

Table 4. Statistical errors of the simulations using four typhoon events.

Station	Typhoon Krosa		Typhoon Fungwong		Typhoon Saola		Typhoon Soulik	
	MAE (m)	RMSE (m)	MAE (m)	RMSE (m)	MAE (m)	RMSE (m)	MAE (m)	RMSE (m)
Taipei Bridge	0.30	0.37	0.19	0.24	0.24	0.29	0.19	0.24
Hsin-Hai Bridge	0.30	0.42	0.15	0.21	0.06	0.08	0.18	0.21
Da-Zhi Bridge	0.23	0.28	0.24	0.33	0.21	0.26	0.13	0.16
Chung-Cheng Bridge	0.22	0.31	0.22	0.29	0.11	0.14	0.17	0.21
Tu-Ti Kung Pi	0.23	0.28	0.07	0.10	0.17	0.22	0.10	0.12
Ru-Kou Yan	0.33	0.42	0.18	0.21	0.40	0.44	---	---

Table 5. Statistical errors between the predicted and observed cumulative probability functions.

Distribution model	Surge height		Astronomical tide		River discharge at Quan-Zean Bridge		River discharge at Fu-Zhou Bridge	
	SE (m)	CC	SE (m)	CC	SE (m^3/s)	CC	SE (m^3/s)	CC
Gumbel	0.0346	0.9806	0.0397	0.9754	6.5460	0.9695	95.6662	0.8605
Weibull	0.0323	0.9848	0.0128	0.9975	2.6015	0.9953	71.7064	0.9354
Frechet	0.1339	0.8880	0.2388	0.8410	10.2649	0.9617	96.7808	0.9557
Normal	0.0663	0.9258	0.0138	0.9971	11.2177	0.9041	122.8602	0.7713
Lognormal	0.0262	0.9901	0.0132	0.9974	7.1395	0.9795	61.7958	0.9578
Log-Pearson 3	0.0268	0.9889	0.0129	0.9975	2.7390	0.9952	68.8232	0.9532

Table 5. Statistical errors between the predicted and observed cumulative probability functions. (Continue)

Distribution model	River discharge at Xiu-Lang Bridge		River discharge at Bao Bridge		River discharge at Jie-Shou Bridge	
	SE (m^3/s)	CC	SE (m^3/s)	CC	SE (m^3/s)	CC
Gumbel	325.3179	0.9761	69.6968	0.9744	109.3666	0.9695
Weibull	321.7177	0.9849	49.0460	0.9895	43.4613	0.9953
Frechet	455.4074	0.9613	945.5690	0.8449	171.4874	0.9617
Normal	548.7033	0.9221	117.6550	0.9195	187.4202	0.9041
Lognormal	403.8747	0.9718	143.3619	0.9739	119.2626	0.9795
Log-Pearson 3	200.0291	0.9911	49.0987	0.9866	45.7697	0.9952

4. Results and Discussion

4.1. Selecting the Best Distribution Function for the Statistical Parameters

Seven parameters, including the astronomical tide and surge height at the mouth of the Danshuei River and the river discharges at the Quan-Zean Bridge, Fu-Zhou Bridge, Xiu-Lang Bridge, Bao Bridge, and Jie-Shou Bridge, are selected for the frequency analysis. The annual maximum for each parameter was adopted to establish the probability density function. The cumulative probability function of each parameter was then determined.

Figure 8 presents the predicted and observed cumulative probability function for each parameter. It shows the predicted cumulative probabilities using different frequency analysis methods, including the Gumbel, Weibull, Frechet, normal, lognormal, and log-Pearson 3

Preprints (www.preprints.org) | NOT PEER-REVIEWED | Posted: 12 March 2018 doi:10.20944/preprints201803.0088.v1

distributions (shown in Table 3). Two indices (i.e., the standard error (SE) and the correlation coefficient (CC)) were used to determine the optimal frequency analysis for each parameter. Table 5 shows statistics for the comparison between the predicted and observed cumulative probabilities for different frequency analysis methods. We found that the optimal frequency analysis methods were the lognormal distribution for surge height, the Weibull distribution for astronomical tide, the Weibull distribution for river discharge at the Quan-Zean Bridge (Taliaokengchi drainage), the lognormal distribution for river discharge at the Fu-Zhou Bridge (Dahan River), the log-Pearson 3 distribution for river discharge at the Xiu-Lang Bridge (Xindian River), the Weibull distribution for river discharge at Bao Bridge (Jingme River), and the Weibull distribution for river discharge at the Jie-Shou Bridge (Keelung River).

Zhong et al. [6] found that the characteristics of high astronomical tide levels at the Hook of Holland could be captured in a normal distribution. The Gaussian copula function presented a dependent structure between the Rhine discharge and the Meuse discharge, where the marginal distributions fit a lognormal distribution for Rhine discharge and a Gamma distribution for Meuse discharge. The best fit for the frequency analysis method is based on the characteristics of each parameter. Therefore, the distribution models for the frequency analysis of astronomical tide and river discharge used in Zhong et al. [6] are quite different from the distribution models adopted in our study.

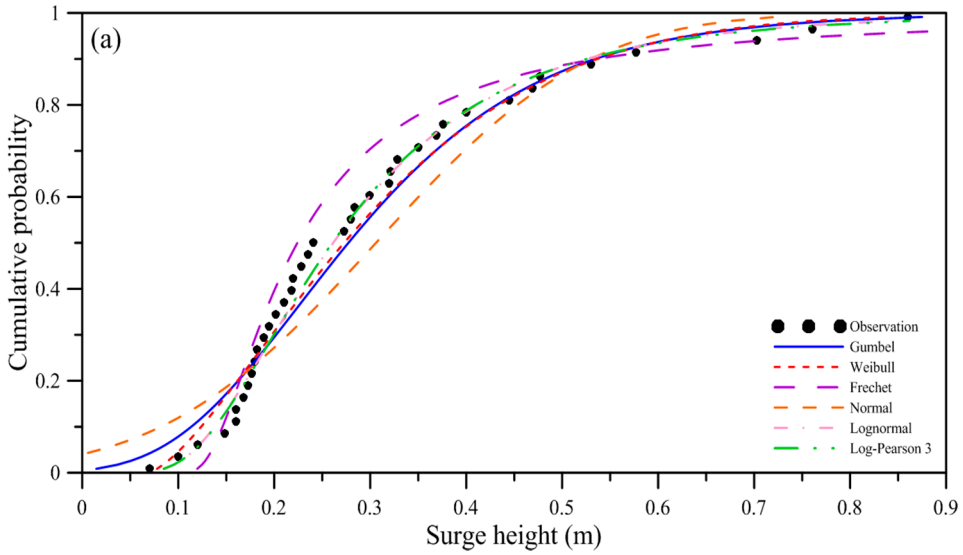

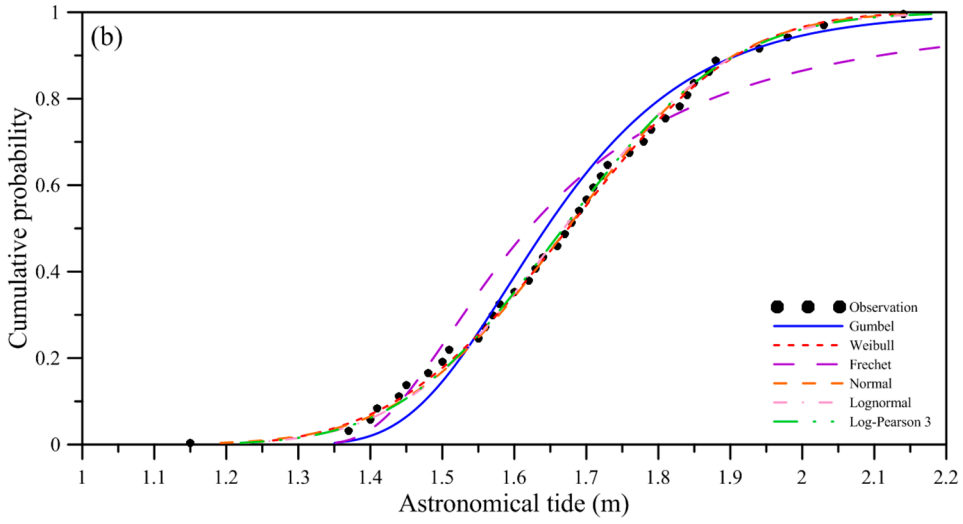

Preprints (www.preprints.org) | NOT PEER-REVIEWED | Posted: 12 March 2018 doi:10.20944/preprints201803.0088.v1

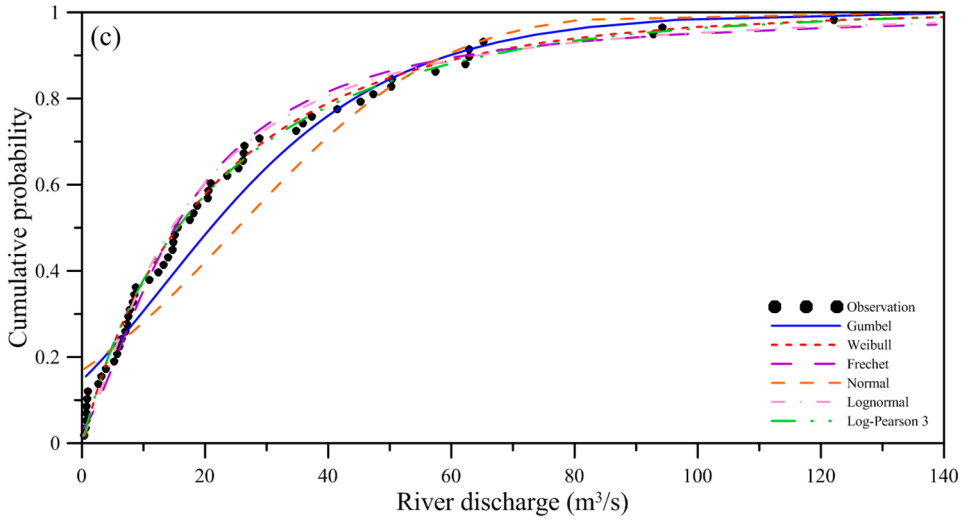

264

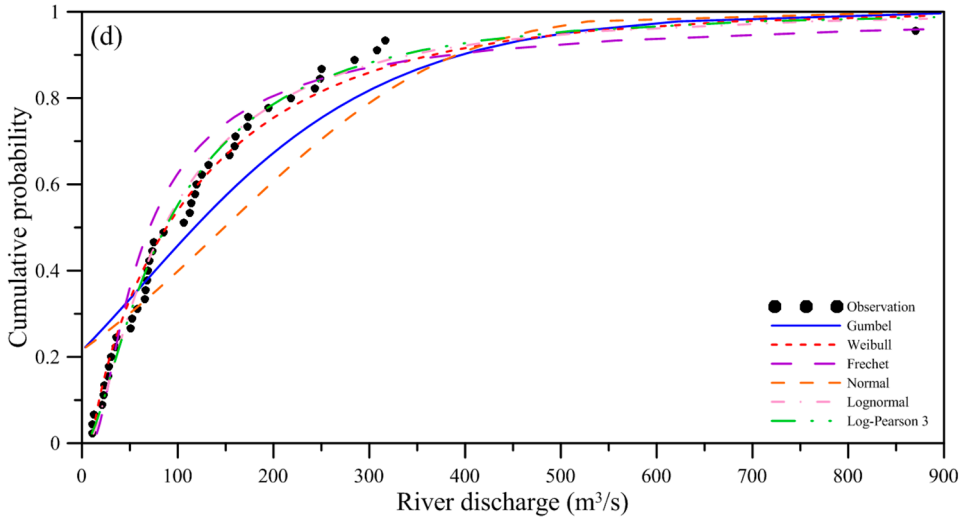

265

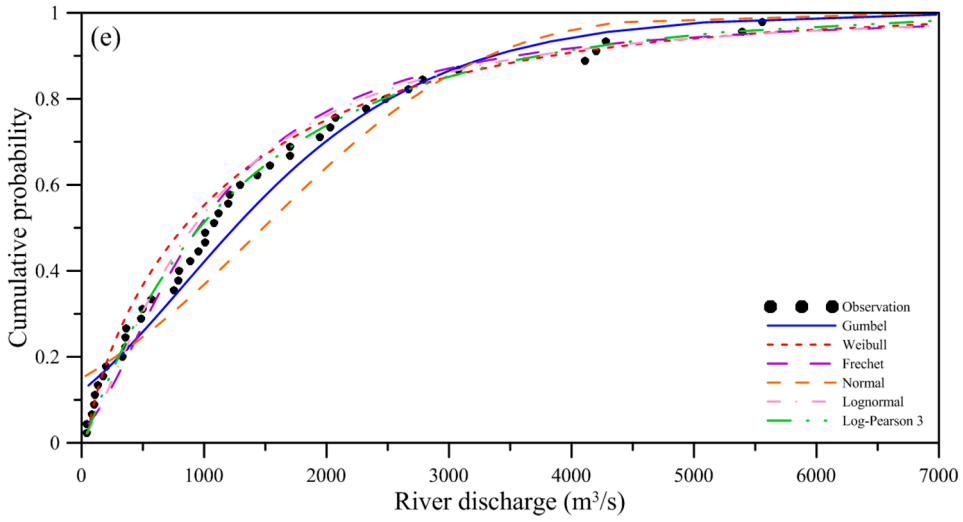

266

Preprints (www.preprints.org) | NOT PEER-REVIEWED | Posted: 12 March 2018 doi:10.20944/preprints201803.0088.v1

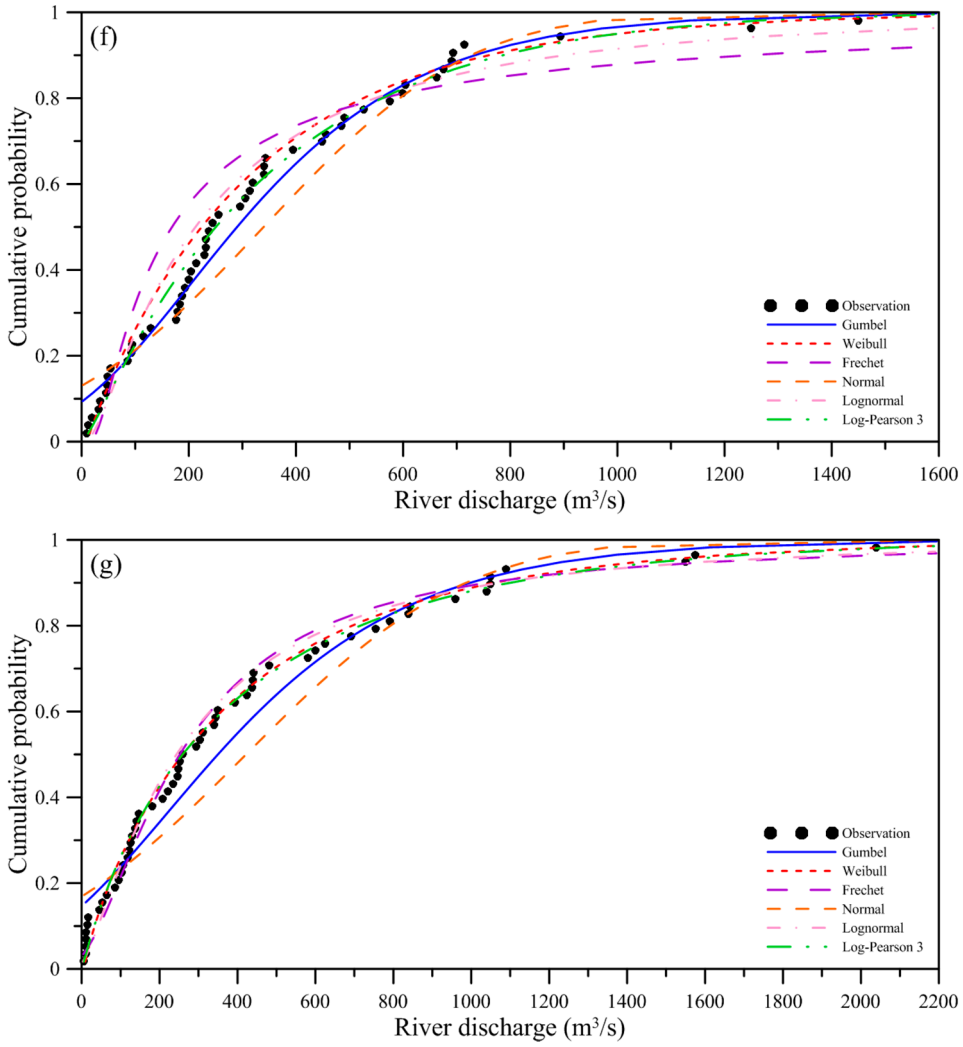

Figure 8. Predicted and observed cumulative probability functions for each of the following parameters: (a) surge height at the mouth of the Danshuei River, (b) astronomical tide at the mouth of the Danshuei River, (c) river discharge at Quan-Zean Bridge (Taliaokengchi drainage), (d) river discharge at Fu-Zhou Bridge (Dahan River), (e) river discharge at Xiu-Lang Bridge (Xindian River), (f) river discharge at Bao Bridge (Jingme River), and (g) river discharge at Jie-Shou Bridge (Keelung River).

4.2. Integrating the Monte Carlo Simulation and the Hydrodynamic Model to Calculate Extreme Water Levels

The joint probability of these seven parameters was used to generate different simulation scenarios. Two thousand scenarios based on the sampled Monte Carlo simulation were generated to drive the validated one-dimensional hydrodynamic model. This means that the Manning friction coefficients (n) in the one-dimensional hydrodynamic model were adopted as shown in Table 1.

Figure 9 presents the cumulative probability function of the water level for different distribution methods at different gauge stations. Gauge stations in the Danshuei River include Guandu Bridge, Taipei Bridge, Hsin-Hai Bridge, Da-Zhi Bridge, and Chung-Cheng Bridge. Table 6 shows statistics for the comparison between the predicted and observed cumulative probabilities at different stations for different frequency analysis methods. The results indicate that the optimal frequency analysis methods are the log-Pearson 3 distribution at Guandu Bridge, the lognormal distribution at Taipei Bridge, the lognormal distribution at Hsin-Hai Bridge, the lognormal distribution at Da-Zhi Bridge, and the Weibull distribution at Chung-Cheng Bridge.

Sindhu and Unnikrishnan [8] estimated the different return periods of extreme events at 26 stations along the east coast of India based on annual maximum sea levels extracted from simulations using a vertically integrated two-dimensional model. The annual maximum sea level fit

Preprints (www.preprints.org) | NOT PEER-REVIEWED | Posted: 12 March 2018 doi:10.20944/preprints201803.0088.v1

290 the Gumbel distribution using the *r*-largest annual maxima method. In our study, we found that the
291 Gumbel distribution was not the best fit for water levels at the five stations.

292 **Table 6.** Statistical errors between the predicted and observed cumulative probability functions at
293 different stations.

Distribution model	Guandu Bridge		Taipei Bridge		Hsin-Hai Bridge		Da-Zhi Bridge		Chung-Cheng Bridge	
	SE (m)	CC	SE (m)	CC	SE (m)	CC	SE (m)	CC	SE (m)	CC
Gumbel	0.0293	0.9939	0.1348	0.9796	0.1704	0.9789	0.2715	0.9504	0.3266	0.9800
Weibull	0.0757	0.9583	0.1650	0.9694	0.1757	0.9783	0.2616	0.9542	0.2355	0.9897
Frechet	0.0590	0.9800	0.1431	0.9778	0.3017	0.9494	0.3565	0.9209	1.7252	0.8140
Normal	0.0416	0.9876	0.2771	0.9142	0.3428	0.9148	0.4296	0.8763	0.5832	0.9365
Lognormal	0.0200	0.9972	0.1061	0.9888	0.1432	0.9852	0.2404	0.9627	0.7784	0.9318
Log-Pearson 3	0.0182	0.9976	0.1105	0.9864	0.1603	0.9817	0.2781	0.9494	0.4557	0.9645

294

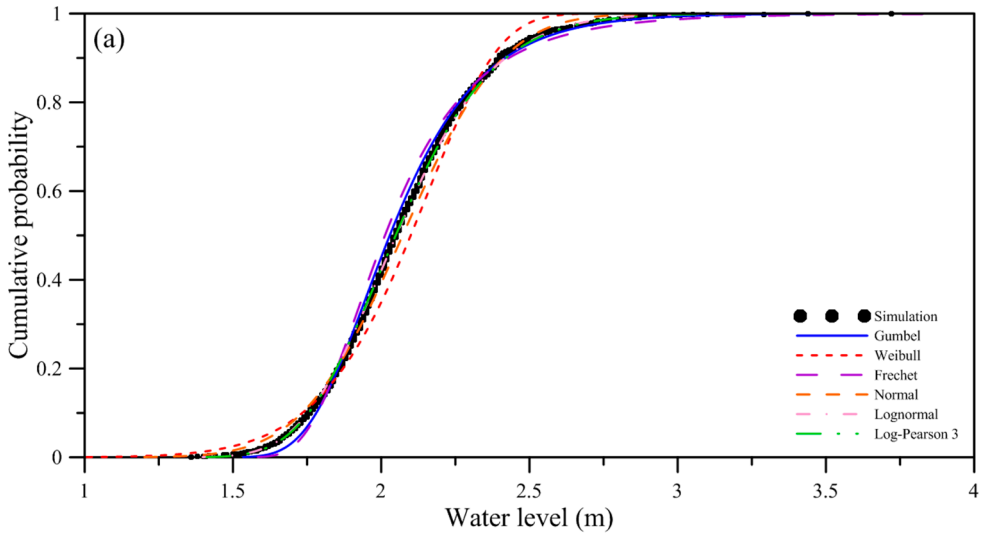

295

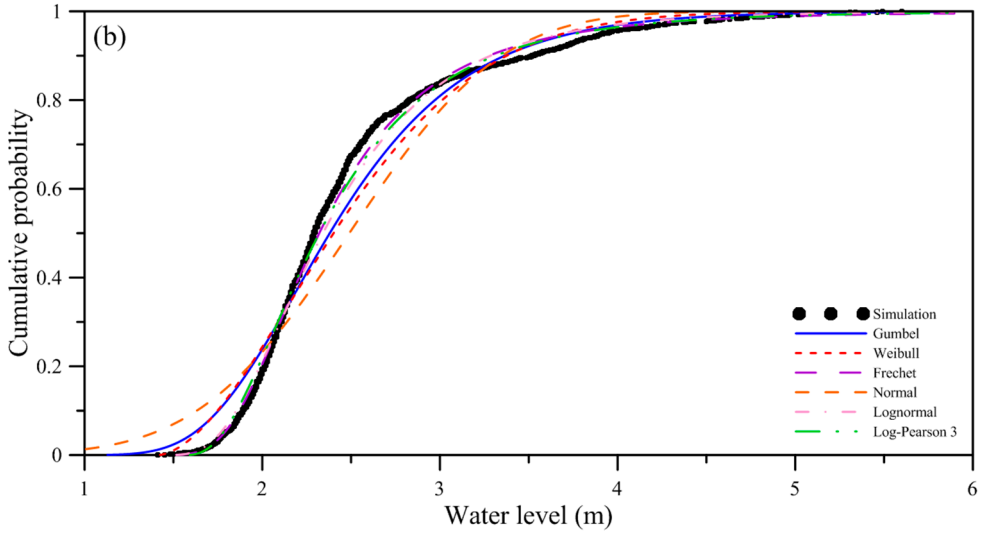

Preprints (www.preprints.org) | NOT PEER-REVIEWED | Posted: 12 March 2018 doi:10.20944/preprints201803.0088.v1

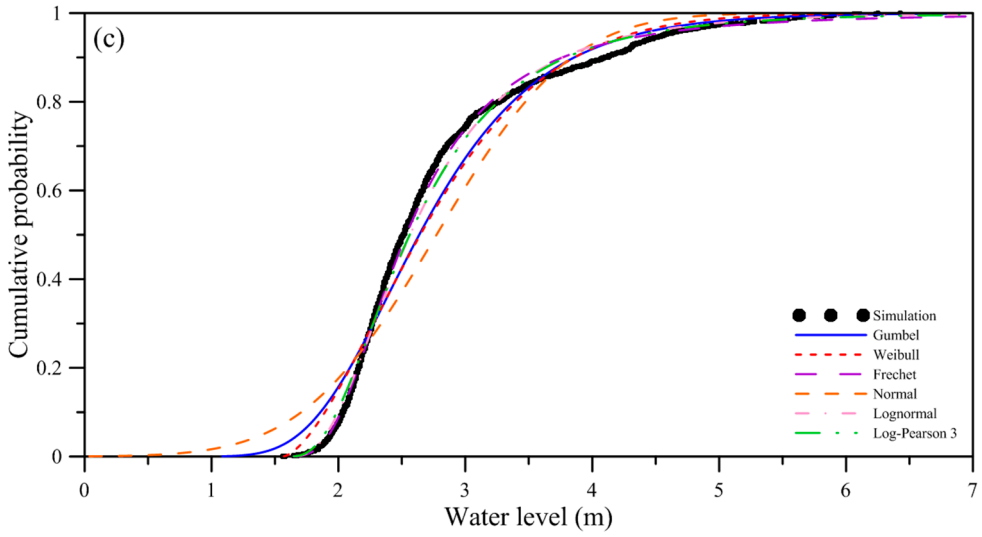

296

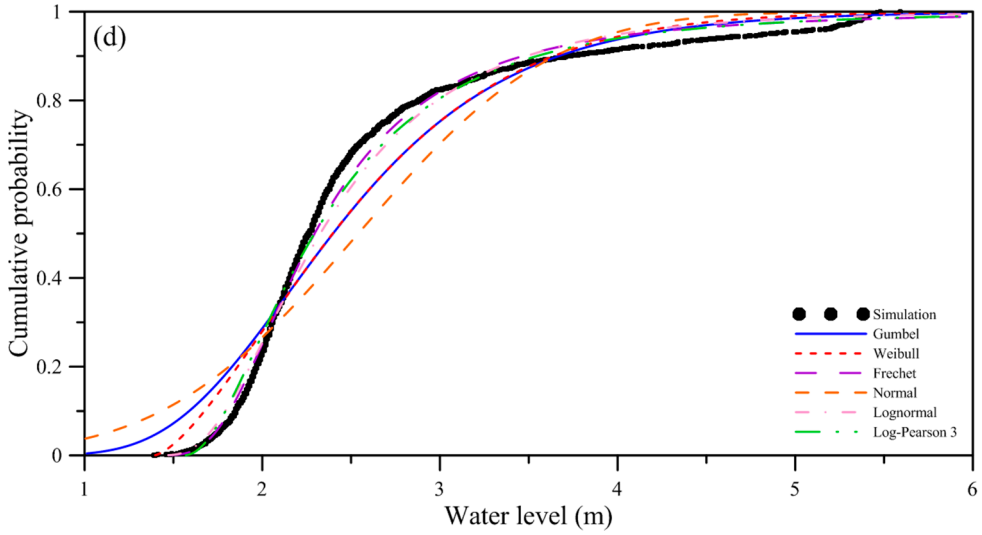

297

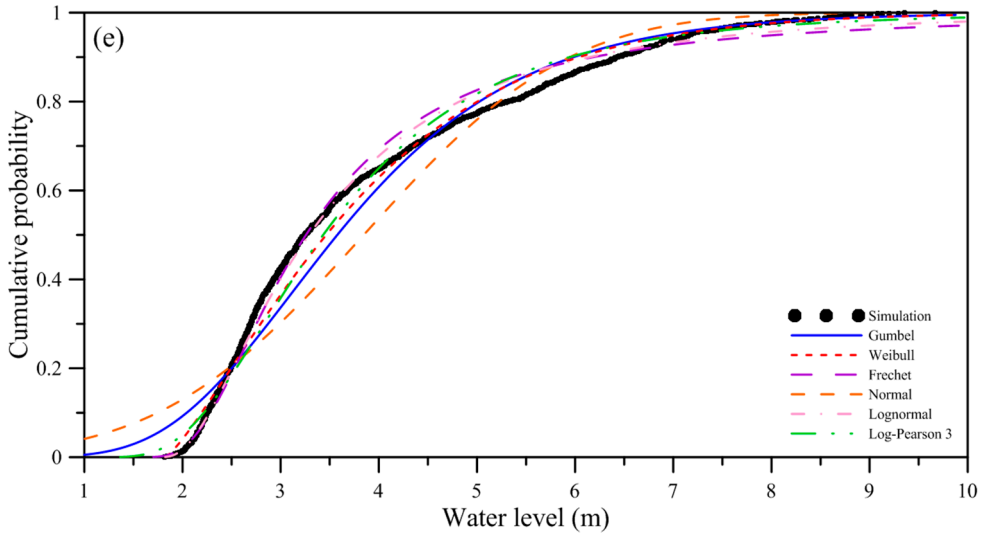

298

299 **Figure 9.** Predicted and observed cumulative probability functions of the water level at (a) Guandu
300 Bridge, (b) Taipei Bridge, (c) Hsin-Hai Bridge, (d) Da-Zhi Bridge, and (e) Chung-Cheng Bridge.

301

 doi:10.20944/preprints201803.0088.v1

4.3. Potential Water Levels for Different Return Periods

The design (extreme) water level is crucial for the design, construction, and maintenance of flood defense systems. According to the Taipei flood control system, the design water level in the Danshuei River system is regarded as the water level with an exceedance frequency of 1/200 (i.e., a 200-year return period). Based on the cumulative probability function of water levels from the frequency analysis, the design water level for different return periods can be yielded. The equation for calculating the water level that corresponds to each return period can be given as follows:

$$T = \frac{1}{1 - F(x)} \tag{7}$$

where T represents the return period, and $F(x)$ is the cumulative probability function.

The design water level can be estimated using different probability distributions from the frequency analysis for different return periods at the five stations based on Eq. (7). Figure 10 presents the predicted water level for the different return periods at five stations. Table 7 shows the design water levels for the different return periods (50, 100, and 200 years). The table indicates that the design water levels for the 200-year return period at Guandu Bridge, Taipei Bridge, Hsin-Hai Bridge, Da-Zhi Bridge, and Chung-Cheng Bridge are 2.90 m, 5.13 m, 6.38 m, 6.05 m, and 9.94 m, respectively. It should be noted that the design water level should be added to the 1.5 m freeboard to result in a projected water level [40].

To avoid extremely high water-levels produced from these extreme events, the construction of new facilities in rivers needs exploration, and the present operational water management system requires adaptation in the future.

Table 7. Design water levels for different return periods.

Return Period	Guandu Bridge (m)	Taipei Bridge (m)	Hsin-Hai Bridge (m)	Da-Zhi Bridge (m)	Chung-Cheng Bridge (m)
50	2.69	4.24	5.08	4.77	8.22
100	2.80	4.68	5.71	5.39	9.09
200	2.90	5.13	6.38	6.05	9.94

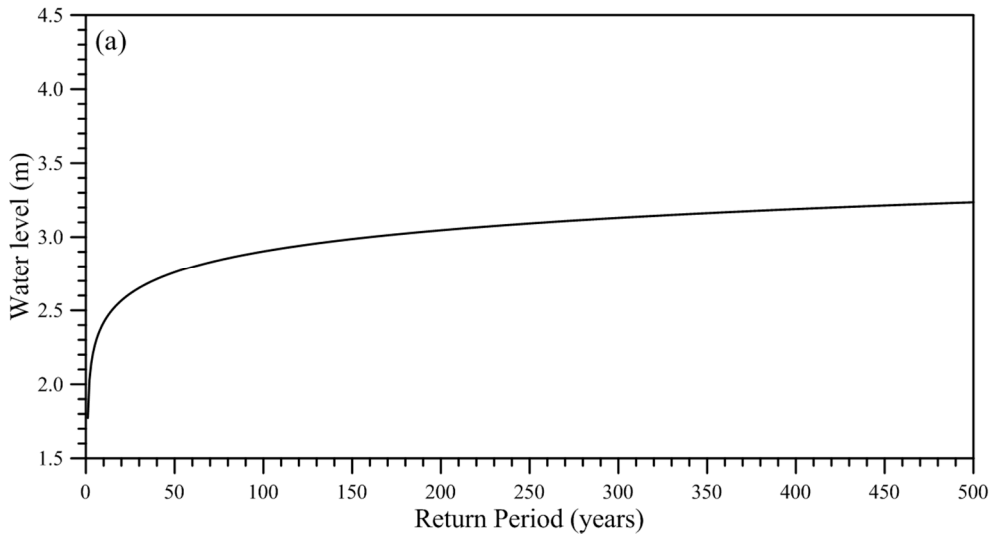

Preprints (www.preprints.org) | NOT PEER-REVIEWED | Posted: 12 March 2018 doi:10.20944/preprints201803.0088.v1

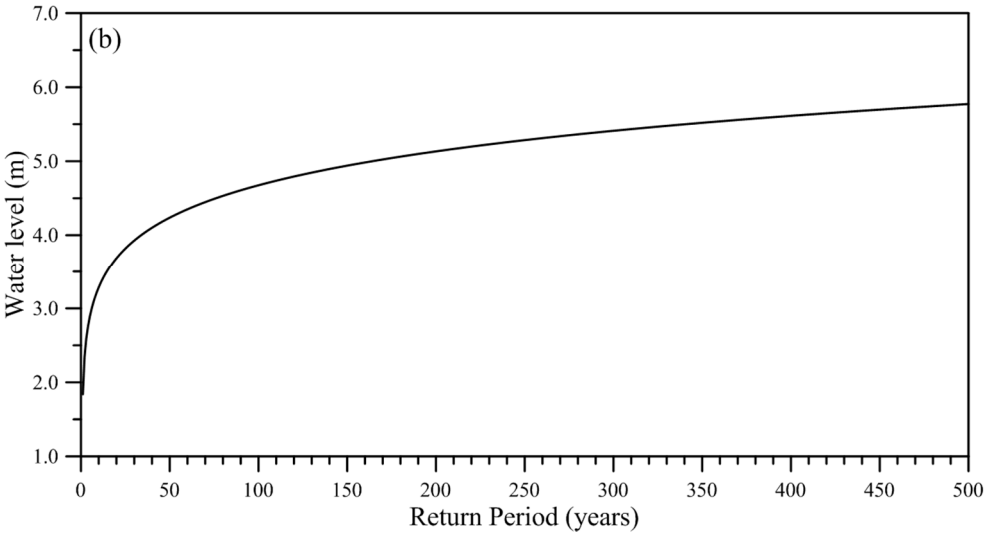

324

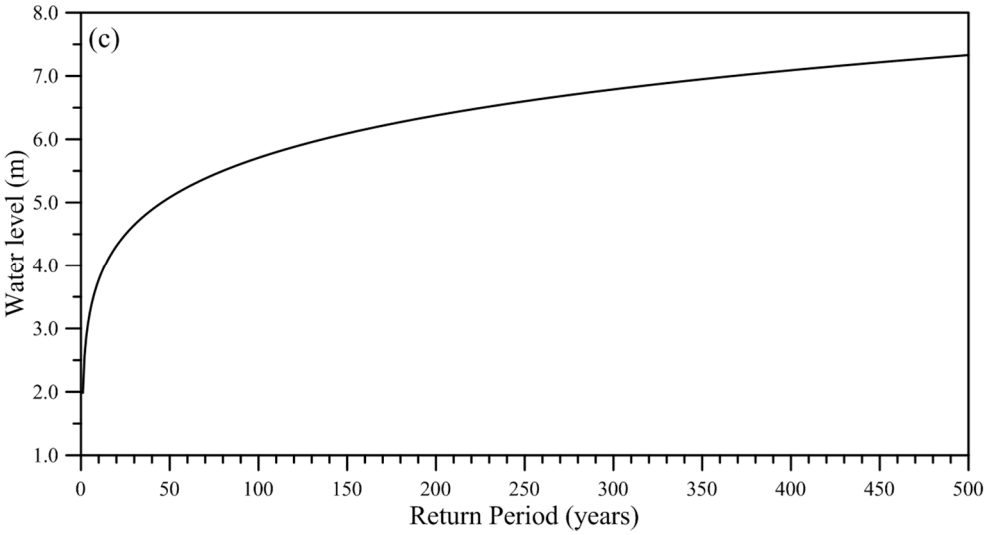

325

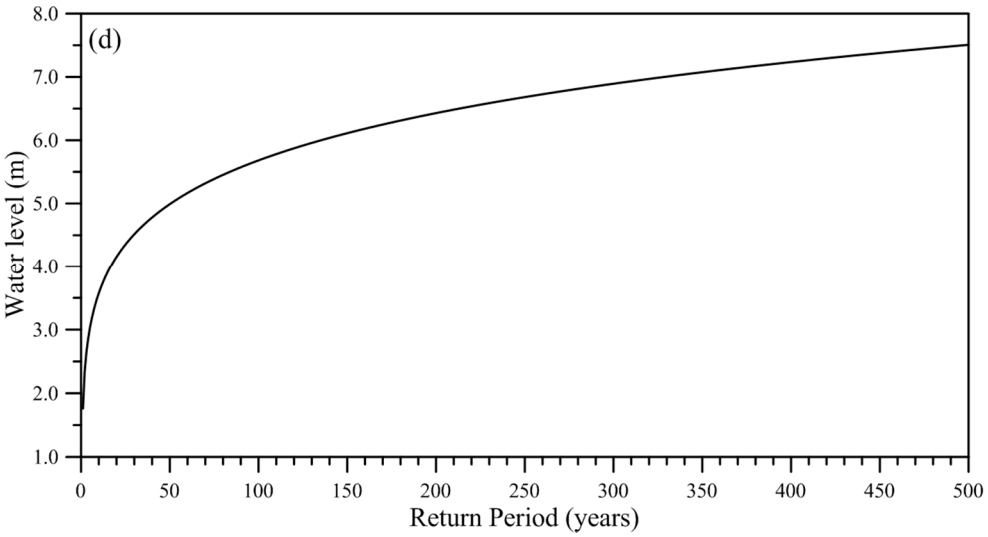

326

Preprints (www.preprints.org) | NOT PEER-REVIEWED | Posted: 12 March 2018 doi:10.20944/preprints201803.0088.v1

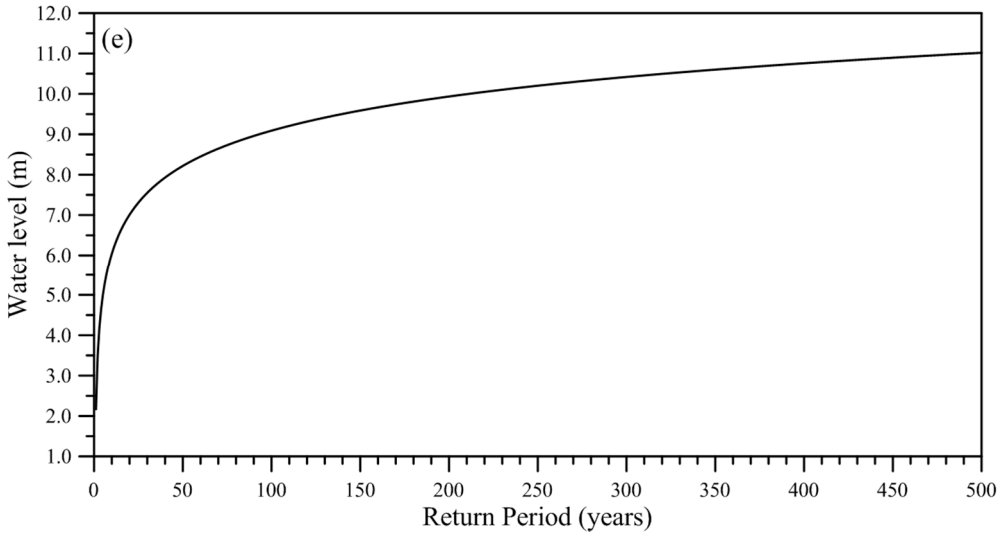

Figure 10. Predicted water levels for different return periods at (a) Guandu Bridge, (b) Taipei Bridge, (c) Hsin-Hai Bridge, (d) Da-Zhi Bridge, and (e) Chung-Cheng Bridge.

5. Conclusions

Recorded historical water levels in the Danshuei River estuarine system of northern Taiwan are not sufficient to perform a traditional frequency analysis directly when predicting extreme water levels. The numerical simulation approach can be adopted when there is not an adequate amount of recorded historical data. This study presents extreme water levels simulated by a stochastic model, which is the integration of the Monte Carlo simulation and a one-dimensional flash flood routing hydrodynamic model. The hydrodynamic model was calibrated and verified with observational water levels using data from four typhoon events. The results indicated a reasonable agreement between the model predictions and recorded observations.

Seven parameters, including the astronomical tide and surge height at the mouth of the Danshuei River and river discharges at Quan-Zean Bridge, Fu-Zhou Bridge, Xiu-Lang Bridge, Bao Bridge, and Jie-Shou Bridge, were selected for the frequency analysis. The joint probability of these seven parameters was used to produce a large set of stochastic scenarios, which were generated by via importance sampling of the Monte Carol simulation. Two thousand scenarios were generated to drive the validated hydrodynamic model simulations. The design water level was estimated using different probability distributions from the frequency analysis for different return periods at the five stations. We found that the design water levels for a 200-year return period at Guandu Bridge, Taipei Bridge, Hsin-Hai Bridge, Da-Zhi Bridge, and Chung-Cheng Bridge were 2.90 m, 5.13 m, 6.38 m, 6.05 m, and 9.94 m, respectively. The estimated design water levels plus the freeboard should be proposed and recommended for engineering design and planning.

In future research, different statistical uncertainties must be investigated. One other issue is that the probability of failure for dikes in river systems should be further considered to understand flood risks.

Acknowledgments: A This research was conducted as part of a grant supported by the Ministry of Science and Technology (MOST) in Taiwan (grant No. 104-2625-M-239-002). The financial support is highly appreciated. The authors would like to express their appreciation to the 10th River Management Bureau and the Water Resources Agency for providing the measurement data.

Author Contributions: Wen-Cheng Liu supervised the progress of the Ministry of Science and Technology, served as a general editor, and prepared a draft of the manuscript. Hong-Ming Liu performed the data collection and analysis, and model establishment and discussed the results with Wen-Cheng Liu. All authors read and approved the final manuscript.

Conflicts of Interest: The authors declare no conflict of interest.

 doi:10.20944/preprints201803.0088.v1

References

1. Zhong, H.; van Gelder, P.H.; Wang, W.; Wang, G.; Liu, Y.; Niu, S. The influence of statistical uncertainty in the hydraulic boundary conditions on the probabilistically computed high water level frequency curve in the Rhine Delta. *Water* **2016**, *8*, 147.
2. LeBlond, P.H. On tidal propagation in shallow rivers. *J. Geophys. Res.* **1978**, *83*, 4717-4721.
3. Godin, G. Modification of river tides by the discharge. *J. Waterw. Port Coast. Ocean Eng. ASCE* **1985**, *111*, 257-274.
4. Pugh, D.T.; Vassie, J.M. Extreme sea levels from tide and surge probabilities. In Proceedings of the 16th Coastal Engineering Conference, Hamburg, American Society of Civil Engineers, Reston, VA., 1979, pp. 911-930.
5. Tawn, J.A.; Vassie, J.M. Extreme sea levels: the joint probability method revisited and revised. *Proc. Inst. Civil Eng.* **1989**, *87*, 429-442.
6. Zhong, H.; van Overloop, P.J.; van Gelder, P.H.A.J.M. A joint probability approach using a 1-D hydrodynamic model for estimating high water level frequencies in the Lower Rhine River. *Nat. Hazard. Earth Syst. Sci.* **2013**, *13*, 1841-1854.
7. Gumbel, E.J. Statistics of Extreme. Columbia University Press, New York, 1985.
8. Sindhu, B.; Unnikrishnan, A.S. Return period estimates of extreme sea level along the east coast of India from numerical simulations. *Nat. Hazard.* **2012**, *61*, 1007-1028.
9. Xu, S.; Huang, W. Frequency analysis for predicting 1% annual maximum water levels along Florida coast, US. *Hydrol. Process.***2008**, *22*, 4507-4518.
10. Huang, W.; Xu, S.; Nnaji, S. Evaluation of GEV model for frequency analysis of annual maximum water levels in the coast of United States. *Ocean Eng.* **2008**, *35*, 1132-1147.
11. Xu, S.; Huang, W. Estimating extreme water levels with long-term data by GEV distribution at Wusong station near Shanghai city in Yangtze Estuary. *Ocean Eng.* **2011**, *38*, 468-478.
12. Mantz, P.A.; Wakeling, H.I. Forecasting flood levels for joint evens of rainfall and tidal surge flooding using extreme value statistics. *Proc. Inst. Civil Eng.* **1979**, *67*, 31-50.
13. Samuels, P.G.; Burt, N. A new joint probability appraisal of flood risk. *Proc. Inst. Civil Eng.- Water Marit. Eng.* **2002**, *154* 109-115.
14. Hsu, M.H.; Fu, J.C.; Liu, W.C. Flood routing with real-time stage correction method for flash flood forecasting in the Tanshui River, Taiwan. *J. Hydrol.* **2003**, *283*, 267-280.
15. Hsieh, L.S.; Hsu, M.H.; Li, M.H. An assessment of structural measures for flood-prone lowlands with high population density along the Keelung River in Taiwan. *Nat. Hazard.* **2006**, *37*, 133-152.
16. Liu, W.C.; Hsu, M.H.; Kuo, A.Y. Investigation of long-term transport in Tanshui River estuary, Taiwan. *J. Waterw. Port Coast. Ocean Eng. ASCE* **2001**, *127*, 61-71.
17. Hsu, M.H.; Kuo, A.Y.; Kuo, J.T.; Liu, W.C. Procedure to calibrate and verify numerical models of estuarine hydrodynamics. *J. Hydraul. Eng. ASCE* **1999**, *125*, 166-182.
18. Liu, W.C.; Hsu, M.H.; Wang, C.R.; Wang, C.F.; Kuo, A.Y. Modeling salt water intrusion in Tanshui River estuarine system—Case-study contrasting now and then. *J. Hydraul. Eng. ASCE* **2004**, *130*, 849-859.
19. Preissman, A. Propagation of translatory waves in channels and rivers. Proceedings 1st Congress of French Association for Computation, Grenoble, France, 1961, pp. 433-442.
20. Amein, M.; Fang, C. Implicit flood routing in natural channel. *J. Hydraul. Div. ASCE* **1970**, *96*, 2481-2500.
21. Liu, W.C.; Wu, C.Y. Flash flood routing modeling for levee-breaks and overbank flows due to typhoon events in a complicated river system. *Nat. Hazard.* **2011**, *58*, 1057-1076.
22. Gelder, P.V.; Neykov, N.M. Regional frequency analysis of extreme water levels along the Dutch coast using L-moments: a preliminary study. In: International scientific conference on stochastic models of hydrological processes and their applications to problems of environmental preservation. Moscow, Russia, 1998, pp. 14-20.
23. Walton, T.L.J. Distribution for storm surge extremes. *Ocean Eng.* **2000**, *27*, 1279-1293.
24. Sobey, R.J. Extreme low and high water levels. *Coast. Eng.* **2005**, *52*, 63-77.
25. Federal Emergency Management Agency (FEMA) of the United States. Final draft guidelines for coastal flood hazard analysis and mapping for the Pacific coast of the United States, 2005.
26. Morrison, J E.; Smith, J.A. Stochastic modeling of flood peaks using the generalized extreme value distribution. *Water Resour. Res.* **2002**, *38*, 41-1-41-12.

27. de Michele, C.; Salvadori, G. Some hydrological applications of small sample estimators of Generalized Pareto and extreme value distributions. *J. Hydrol.* **2005**, *301*, 37-53.
28. Kroese, D.P.; Brereton, T.; Taimre, T.; Botev, Z.I. Why the Monte Carlo method is so important today. *WIREs Comput. Stat.***2014**, *6*, 386-392.
29. de Moel, H.; Asselman, N.E.M.; Aerts, J.C.J.H. Uncertainty and sensitivity analysis of coastal flood damage estimates in the west of the Netherlands. *Natural Hazards and Earth System Sciences* **2012**, *12*, 1045-1058.
30. Camacho, R.A.; Martin, J.L. (2013) Bayesian Monte Carlo for evaluation of uncertainty in hydrodynamic models of coastal system. *J. Coast. Res.* **2013**, *SI 65*, 886-891.
31. Lopeman, M.; Deodatis, G.; Franco, G. Extreme storm surge hazard estimation in low Manhattan. *Nat. Hazard.* **2015**, *78*, 355-391.
32. Hollt, T.; Altaf, M.U.; Mandli, K.T.; Hadwiger, M.; Dawson, C.N.; Hoteit, I. Visualizing uncertainties in a storm surge ensemble data assimilation and forecasting system. *Nat. Hazard.* **2015**, *77*, 317-336.
33. van Bijnen, N.; Korving, H.; Clements, F. Impact of sewer condition on urban flooding: an uncertainty analysis based on field observations and Monte Carlo simulations on full hydrodynamic models. *Water Sci. and Technol.* **2012**, *65*, 2219-2227.
34. Dimitriadis, P.; Tegos, A.; Oikonomou, A.; Pagana, V.; Koukouvino, A.; Mamassis, N.; Koutsoyiannis, D.; Efstratiads, A. Comparative evaluation of 1D and quasi-2D hydraulic models based on benchmark and real-world applications for uncertainty assessment in flood mapping. *J. Hydrol.* 2016, *534*, 478-492.
35. Kottegoda, N.T.; Natale, L.; Raiteri, E. Monte Carlo simulation of rainfall hyetographs for analysis and design. *J. Hydrol*. **2014**, *519*, 1-11.
36. Nakan, K.; Haidary, A. Sensitivity analysis of stream water quality and land cover linkage models using Monte Carlo method. International *J. Environ. Res.* **2012**, *4*, 121-130.
37. Martin, C.; Ayesa, E. An integrated Monte Carlo methodology for the calibration of water quality models. *Ecol. Model*. **2010**, *221*, 2656-2667.
38. Jiang, Y.; Nan, Z.; Yang, S. Risk assessment of water quality using Monte Carlo simulation and artificial neural network method. *J. Environ. Manage.* **2013**, *122*, 130-136.
39. Antanasijevic, D.; Pocajt, V.; Peric-Grujic, A.; Ristic, M. Modelling of dissolved oxygen in the Danube River using artificial neural networks and Monte Carlo Simulation uncertainty analysis. *J. Hydrol.* **2014**, *519*, 1895-1907.
40. Water Resources Agency. Flood Disaster Prevention Business Plan. Water Resource Agency, Ministry of Economic Affairs, 2011.